Development of a Land Surface Model. Part II: Data Assimilation

JONATHAN E. PLEIM*

Atmospheric Sciences Modeling Division, Air Resources Laboratory, National Oceanic and Atmospheric Administration, Research Triangle Park, North Carolina

AIJUN XIU+

Environmental Programs, MCNC–North Carolina Supercomputing Center, Research Triangle Park, North Carolina

(Manuscript received 9 January 2003, in final form 10 June 2003)

ABSTRACT

Part I described a land surface model, its implementation in the fifth-generation Pennsylvania State University–National Center for Atmospheric Research Mesoscale Model (MM5), and some model evaluation results. Part II describes the indirect soil moisture data assimilation scheme. As described in Part I, the land surface model includes explicit soil moisture, which is based on the Interactions between Soil, Biosphere, and Atmosphere (ISBA) model, and three pathways for evaporation: soil evaporation, evaporation from the wet canopy, and vegetative transpiration. The data assimilation scheme presented here also follows similar work on data assimilation for ISBA and uses model biases of the 2-m air temperature and humidity against observed analyses to nudge soil moisture. An important difference from the ISBA schemes is that the nudging strengths are computed from model parameters such as solar radiation, temperature, leaf area, vegetation coverage, and aerodynamic resistance rather than from statistically derived functions. The rationale is that nudging soil moisture according to model biases in air temperature and humidity should depend on the degree of coupling across the land–atmosphere interface. Thus, nudging strengths are designed to reflect the potential for the surface and root-zone soil moisture to affect near-surface air temperature and humidity. Model test cases are used to examine relationships between the nudging strengths and modeled physical parameters and then to demonstrate the effects of the nudging scheme on model results.

1. Introduction

Realistic simulation of land surface processes is well known to be of critical importance for atmospheric modeling. A number of land surface models (LSMs) have been developed in recent years, first for application in general circulation models, in which long-term energy and moisture budgets are the key issues, and more recently in mesoscale meteorological models, in which local variations in temperature and moisture can have important effects on mesoscale weather. In addition to weather forecasting, mesoscale models are also used as parts of atmospheric-chemistry modeling systems in which long-term and episodic-type simulations are used to study pollutant levels and design emission control strategies. Land surface processes directly affect several parameters crucial for air-quality applications, such as ground-level temperature and the temporal variation of the planetary boundary layer (PBL) height. Because most air-quality modeling studies are generally conducted in the retrospective mode, data assimilation and realistic description of seasonal vegetation changes are important aspects of the land surface modeling system for long-term simulations.

The difficulty in the initialization of soil moisture fields over mesoscale or regional domains and the inability of simple soil moisture models to track realistically the long-term evolution of soil moisture fields suggest the need for some kind of data assimilation for dynamical adjustment of soil moisture fields (Chen and Dudhia 2001). The assimilation scheme described here uses errors in the predicted values of 2-m temperature and relative humidity as compared with gridded analyses of surface-based observations. These errors are used to nudge root-zone and surface soil moisture. The concept is that errors is low-level temperature and humidity may be due to erroneous partitioning of surface latent and sensible heat fluxes, which, in turn, may be

* Additional affiliation: National Exposure Research Laboratory, U.S. Environmental Protection Agency, Research Triangle Park, North Carolina.

+ Current affiliation: Carolina Environmental Program, University of North Carolina at Chapel Hill, Chapel Hill, North Carolina.

Corresponding author address: Jonathan E. Pleim, U.S. EPA, Mail Drop E243-03, Atmospheric Modeling Division, Research Triangle Park, NC 27711.
E-mail: pleim@hpcc.epa.gov

caused by unrealistic representation of soil moisture conditions.

Although critically important to surface exchange processes, soil moisture is very difficult to initialize accurately because of the lack of widespread measurements and the high degree of spatial variability. A common approach to this problem is to ''spin up'' the model for a few weeks or longer to allow the model's own precipitation, evaporation, and evapotranspiration processes to create realistic soil moisture fields. A drawback of this approach is that modeled precipitation fields, as well as cloud cover and many other modeled fields, contain inevitable errors. Also, LSMs simple enough to be included in mesoscale grid models cannot be relied upon to track long-term trends in soil moisture realistically. Thus, soil moisture is an obvious candidate for dynamic adjustment, but not by direct assimilation of observations given that widespread operational measurements of soil moisture are not generally available, especially at root depths. Indirect nudging depends on strong coupling between soil moisture and near-surface temperature and humidity through evaporation and evapotranspiration. Thus, the nudging coefficients must be carefully prescribed to act only when and where this coupling is strong so that soil moisture nudging is not done when model errors are attributable to other causes.

Pleim and Xiu (1995) described a one-dimensional prototype of the Pleim–Xiu land surface model (PX LSM). In Part I, Xiu and Pleim (2001, hereinafter XP01) described its implementation in the fifth-generation Pennsylvania State University–National Center for Atmospheric Research Mesoscale Model (MM5; Grell et al. 1994). Because the PX LSM was originally based on the Interactions between Soil, Biosphere, and Atmosphere (ISBA) model, the idea for the assimilation scheme in the PX LSM also follows the assimilation schemes developed for the ISBA model. Soil moisture assimilation from analyses of near-surface meteorological parameters for the ISBA model has been under development for many years. Mahfouf (1991) described a one-dimensional feasibility study, followed by further development (Bouttier et al. 1993a) and implementation in a 3D mesoscale meteorological model (Bouttier et al. 1993b). In more recent work, Giard and Bazile (2000) described a similar soil moisture assimilation technique applied to a global NWP model. All of these studies employed sequential assimilation of soil moisture at 6-h intervals based on forecast errors derived from the differences between simulated 2-m air temperature and relative humidity and analyzed fields based on observations. Corrections to the surface soil layer Δw_g and deep soil layer Δw_2 are determined by

$$\Delta w_g = \alpha_1(T^a - T^f) + \alpha_2(\mathrm{RH}^a - \mathrm{RH}^f) \quad \text{and} \quad (1)$$

$$\Delta w_2 = \beta_1(T^a - T^f) + \beta_2(\mathrm{RH}^a - \mathrm{RH}^f), \quad (2)$$

where the a and f superscripts on temperature T and relative humidity RH indicate analysis and forecast, respectively. Mahfouf (1991) used optimal interpolation (OI) to estimate the assimilation weights α and β from a set of 1D Monte Carlo simulations. Bouttier et al. (1993a) suggested a set of analytical expressions for the assimilation coefficients dependent on vegetation coverage, local solar time, minimum stomatal resistance, leaf area index (LAI), and soil texture to facilitate application in operational 3D models. Giard and Bazile (2000) rederived a set of polynomial functions to provide a better fit to the original assimilation coefficients developed by Mahfouf (1991). Douville et al. (2000) compared this OI scheme with the simple nudging scheme used operationally at the European Centre for Medium-Range Weather Forecasts (ECMWF). They found significant advantage to the OI scheme because of both the varying assimilation strengths and the use of 2-m temperature in addition to the 2-m humidity used by the ECMWF scheme. Note that ECMWF has since adopted the OI sequential assimilation scheme for operational use.

The technique described in this paper follows a similar approach for nudging soil moisture according to functions of model parameters such as insolation, air temperature, leaf area, soil texture, vegetation coverage, and aerodynamic resistance in order to nudge most strongly when surface–atmosphere coupling is greatest. A drawback to this approach is that it may cause changes in soil moisture when the atmospheric model's errors are unrelated to surface fluxes. However, the magnitude of the assimilation coefficients is small when compared with physical forcings, and it takes several days to produce large changes in soil moisture. Thus, short-term errors caused by unrelated phenomena, such as mistiming of frontal passages or erroneous predictions of cloud cover, usually have minimal impact on soil moisture adjustment.

This is the second in a series of papers describing a land surface and PBL modeling system that has been applied to mesoscale meteorological and mesoscale atmospheric-chemistry modeling. Part I (XP01) provides a thorough description of the land surface model as applied in MM5 as well as some initial episodic evaluation through comparison with measurements from the First International Satellite Land Surface Climatology Project (ISLSCP) Field Experiment (FIFE)-87 field study. In Part II, we focus on the soil moisture nudging scheme, which we consider to be an essential component of the LSM system, especially for long-term retrospective modeling studies typical of air-quality applications. After a brief review of the LSM formulation in section 2, a technical description of the soil moisture data assimilation scheme is presented in section 3. Section 4 demonstrates the sensitivity of the nudging strength and forcing terms to various model parameters such as solar radiation and turbulent transport. An evaluation of the efficacy of the nudging scheme is presented through a comparison with observations in section 5. A few concluding remarks are offered in section 6.

2. Land surface model overview

Because the PX LSM was described in detail in Part I, only a brief review of the model formulation is presented here. The land surface model's key elements are a surface model including soil moisture and evapotranspiration based on the ISBA model (Noilhan and Planton 1989, hereinafter NP89), and a nonlocal closure PBL model developed by Pleim and Chang (1992). The surface model includes a two-layer soil model with a 1-cm surface layer and a 1-m root-zone layer. Evaporation has three pathways: direct soil surface evaporation, vegetative evapotranspiration, and evaporation from wet canopies. Ground surface temperature is computed from the surface energy balance using a force–restore algorithm for heat exchange within the soil. Stomatal conductance is parameterized according to root-zone soil moisture, air temperature and humidity, photosynthetically active radiation (PAR), and several vegetation parameters such as LAI and minimum stomatal resistance. The functional forms of these parameterizations have been significantly modified from the original ISBA model, as described in XP01. A simple parameterization for describing the seasonal growth of vegetation, including leaf-out and leaf-drop of deciduous trees, has also been developed and tested. An adjunct chemical dry deposition model that uses the canopy and aerodynamic resistances directly from this LSM has been developed and evaluated against field measurements (Pleim et al. 2001). The model also includes a data assimilation scheme, similar to the technique described by Bouttier et al. (1993a), which is the primary topic for this paper.

a. Land surface model

The five partial differential equations for surface soil temperature, deep soil temperature (a slowly varying reservoir with a timescale of 10 days), soil moisture in the surface layer (1 cm) and root zone (1 m), and canopy moisture (dew and intercepted rain) are shown in Eqs. (1)–(5) of Pleim and Xiu (1995); these equations are essentially the same ones originally presented by NP89. Total evaporation is the sum of evaporation from the soil E_g, wet canopies E_r, and evapotranspiration $E_{\rm tr}$. In highly vegetated areas, surface moisture flux is generally dominated by $E_{\rm tr}$. The key parameter for realistic simulation of evapotranspiration is the canopy resistance R_c:

$$R_c = \frac{R_{\rm stmin}}{F_1(\rm PAR)F_2(w_2)F_3(\rm RH_s)F_4(T_a)\rm LAI}, \qquad (3)$$

where F_1–F_4 are empirical stress functions of PAR, root-zone soil moisture w_2, relative humidity at the leaf surface $\rm RH_s$, and air temperature T_a. The minimum stomatal resistance $R_{\rm stmin}$ is specified according to vegetative species as shown in XP01. Note that the scaling up from leaf to canopy appears from Eq. (3) to be simply a linear dependence on LAI. There is, however, an additional dependence on LAI in the F_1 term that accounts for increased shading in denser canopies (Jacquemin and Noilhan 1990).

All four empirical stress functions have been updated from NP89 both to smooth their effects and to give better results, as presented in XP01. For example, changes to $F_3(\rm RH_s)$ are the most significant departure from NP89. Pleim (1999) showed that using a function of relative humidity at the surface of the leaf gives a more realistic response of stomatal conductance to changes in ambient temperature and humidity than using functions of the ambient vapor pressure deficit.

b. PBL model

The PX LSM option in MM5 includes a PBL model known as the Asymmetric Convective Model (ACM), developed by Pleim and Chang (1992). ACM is a derivative of the Blackadar convective model (Blackadar 1978) in that it uses the same nonlocal upward transport that is intended to mimic rising buoyant convective plumes. It also uses a similar closure assumption for defining the mixing rate based on a quasi-equilibrium balance of surface sensible heat flux with internal PBL mixing. The primary difference from the Blackadar model is that the downward transport is local, layer by layer, to simulate compensatory subsidence in convective boundary layers. In addition, the eddy diffusivity functions for nonconvective conditions and the flux-profile functions and parameterizations have been recently updated (Pleim and Xiu 2001). The PBL height is calculated using the bulk Richardson number as suggested by Holtslag et al. (1995). Note that, even though the ACM is used here as the PBL model, the land surface model could be coupled with any other PBL model available in the MM5 system, such as the Blackadar PBL scheme, the Medium-Range Forecast Model scheme, or the Burk–Thompson turbulent kinetic energy scheme.

3. Technical description

The soil moisture assimilation technique developed for this model differs from the techniques used with the ISBA model in two ways. First, rather than applying incremental periodic adjustments to the soil moisture [Eqs. (1) and (2)], we use continuous Newtonian relaxation or ''nudging'' [see Stauffer and Seaman (1990) for an overview of Newtonian relaxation]. Second, nudging coefficients are defined according to model parameters rather than from statistical analysis. The nudging soil moisture tendencies are

$$\frac{\partial w_g}{\partial t} = \alpha_1(T^a - T^f) + \alpha_2(\rm RH^a - RH^f) \quad \text{and} \qquad (4)$$

$$\frac{\partial w_2}{\partial t} = \beta_1(T^a - T^f) + \beta_2(\rm RH^a - RH^f). \qquad (5)$$

Soil moisture tendencies are evaluated every model time step using the current forecast values of T and RH as compared with ''observed'' values interpolated from periodic (usually 3 hourly) objective analyses. When the deep soil moisture w_2 exceeds the field capacity, further moistening by nudging is not permitted but drying is. In a similar way, when w_2 falls below the wilting point, only nudging in the moistening direction is allowed. These restrictions prevent runaway moistening or drying when model biases do not respond to soil moisture adjustments.

As an alternative to the OI analyses described by Mahfouf (1991) and others, the nudging coefficients ($\alpha_{1,2}$ and $\beta_{1,2}$) are defined as combinations of relevant model parameters. The rationale guiding these parameterizations is the inclusion of the major factors that influence the coupling between the soil layers and the lowest atmospheric layer. The surface soil layer (1 cm) nudging coefficients act on the nonvegetated fractional area (1 − veg) and are proportional to surface insolation R_g:

$$\alpha_{1,2} = A_{1,2}\frac{R_g}{S}F_{\text{txt}}\frac{R_{a\text{min}}}{R_a}(1 - \text{veg}), \tag{6}$$

where

$$F_{\text{txt}} = \frac{w_{\text{wlt}}(\text{stype}) + w_{\text{fc}}(\text{stype})}{w_{\text{wlt}}(\text{loam}) + w_{\text{fc}}(\text{loam})}$$

adjusts for different soil texture types (stype), S is the solar constant (1370 W m^{-2}), R_a is the aerodynamic resistance [as defined in Eq. (5) of Part I], $R_{a\text{min}}$ is a minimum aerodynamic resistance set to 10 s m^{-1}, w_{wlt} is the soil moisture at wilting point, and w_{fc} is the soil moisture at field capacity. The deep-soil-layer (1 m) nudging coefficients, which act on the vegetated fractional area (veg), are related to the canopy conductance without the functional dependence on soil moisture and air humidity:

$$\beta_{1,2} = B_{1,2}\frac{R_{c\text{min}}F_1F_4\text{LAI}}{R_{\text{stmin}}}F_{\text{txt}}\frac{R_{a\text{min}}}{R_a}\text{veg}, \tag{7}$$

where F_1, F_4, LAI, and R_{stmin} are all parameters used to estimate canopy conductance as shown in Eq. (3). A minimum canopy resistance ($R_{c\text{min}} = 30$ s m^{-1}) is included to normalize the canopy conductance term to order 1. Note that two of the four stomatal stress functions for insolation and air temperature are included but that the other two for soil moisture and air humidity are not. The dependences on soil moisture and air humidity are excluded to avoid asymmetrical responses. Initial experiments using the full canopy conductance ($1/R_c$) showed a tendency toward increasing soil dryness over several days. Whenever model errors in temperature and humidity forced a drying nudging tendency, canopy conductance is decreased. Thus, when subsequent model errors forced a moistening nudging tendency, the nudging strength, which was proportional to canopy conductance, was less. Over several days the entire deep soil moisture field was driven to very dry values and could not recover. Another reason for exclusion of the humidity stomatal function is that the partial stomatal shutdown at low relative humidities is largely compensated by the high vapor pressure deficit that drives the moisture flux.

Common elements of the soil moisture nudging coefficients for both surface and deep soil layers include dependence on the degree of atmospheric turbulence, as indicated by the aerodynamic resistance, and scaling by the soil texture (F_{txt}), which follows soil texture adjustments suggested by Bouttier et al. (1993a). The constants $A_{1,2}$ and $B_{1,2}$ are designed to result in maximum magnitudes for the nudging coefficients ($\alpha_{1,2}$ and $\beta_{1,2}$) similar to Bouttier et al. (1993a) and Giard and Bazile (2000):

$$A_1 = \frac{-10^{-4}}{6\text{ h}}(\text{K}^{-1}), \qquad A_2 = \frac{10^{-5}}{6\text{ h}},$$

$$B_1 = \frac{-1.5 \times 10^{-2}}{6\text{ h}}(\text{K}^{-1}), \quad \text{and} \quad B_2 = \frac{10^{-3}}{6\text{ h}}.$$

The strength of the nudging and the timescale of its effects are controlled by the magnitude of these coefficients [note that the values are presented for 6-h intervals for comparison with Bouttier et al. (1993a)]. The coefficients for shallow soil moisture nudging (A_1 and A_2) are about two orders of magnitude smaller than the deep soil coefficients (B_1 and B_2). Thus, the scheme is designed primarily to affect deep soil moisture, which has a long timescale (several days to weeks) and dominates the partitioning of surface fluxes in vegetated areas. The shallow soil nudging has very little effect in vegetated areas and is included mainly to allow for some nudging in sparse vegetation or nonvegetated areas. The small magnitudes of these coefficients select for very persistent biases that allow some small influence of the deep soil moisture through the diffusive connection between soil layers.

The coefficients for temperature were originally specified to be one order of magnitude less and are of opposite sign to the coefficients for humidity. The sign accounts for the direction of nudging with respect to the sign of the bias. When modeled temperature is too high, the nudging moistens the soil—hence, the negative sign. When the humidity is too high, the nudging dries the soil—hence, the positive sign. The order-of-magnitude ratio specifies that 1 K of temperature bias will have the same effect as a 10% relative humidity bias, which is similar to the ratio of OI coefficients derived by Mahfouf (1991) for highly vegetated areas. Note that we have recently altered this relationship by increasing B_1 by 50% to give greater weight to temperature biases because ground-level air temperature is generally more important than relative humidity in air-quality modeling applications.

The combination of the temperature and humidity

terms helps to select for situations in which the biases are related to the partitioning between surface sensible and latent heat fluxes. In general, when deep soil moisture is too high (or too low), the latent heat flux is too high (or too low) and sensible heat flux is too low (or too high), leading to wet (or dry) and cool (or warm) biases. In these situations, the temperature and humidity nudging terms work together to nudge soil moisture. When errors are due to other causes, the biases may not have opposite signs, and so the nudging terms tend to oppose each other. Boosting B_1 by 50%, however, has the effect of increasing the response to temperature bias regardless of the cause.

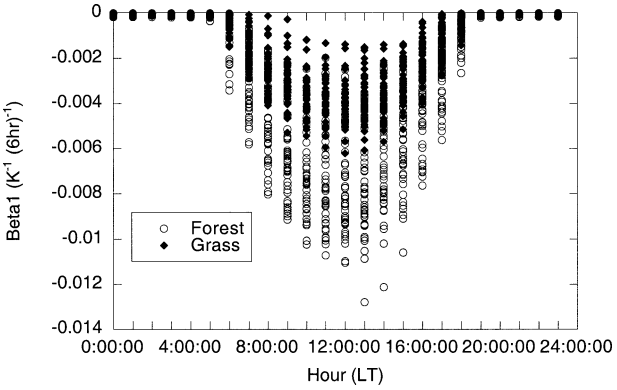

FIG. 1. Deep soil moisture nudging strength for temperature (β_1) by time of day for two sites.

4. Sensitivity

The following sensitivity and evaluation experiments are derived from a series of MM5 runs using the PX LSM with the soil moisture nudging scheme for 11 June–26 July 1999. MM5, version 3.4, was configured with 32-km horizontal grid dimensions covering the entire contiguous United States and 30 vertical layers, with the midpoint of the lowest layer at about 19 m AGL. Other physics options include the Rapid Radiative Transfer Model (RRTM) radiation scheme (Mlawer et al. 1997), the Reisner I mixed-phase microphysics (Reisner et al. 1998), and the Kain–Fritsch convective scheme (Kain and Fritsch 1990, 1993). Analysis-based four-dimensional data assimilation was used for winds at all levels and temperature and humidity above the PBL, following Stauffer et al. (1991). Upper-air analyses were every 12 h, and surface analyses were every 3 h. Objective analyses of 2-m temperature and humidity are produced in the MM5 system using a modified Cressman technique with ''banana shaped'' weighting functions (Benjamin and Seaman 1985). Note that the sensitivity and evaluation analyses presented here focus on the deep-soil-moisture nudging according to temperature biases.

Assimilation functions

Detailed time series model output was extracted for several grid cells for analyses and comparison with observations. Figure 1 shows scatterplots of the deep-soil nudging coefficient for air temperature (β_1) computed according to Eq. (7) versus hour (LT) for a grass site and a forest site, both in central Tennessee, for the full time period. The most obvious feature of these plots is that the maximum (negative) values closely follow the solar diurnal pattern. The reasons are both the direct influence of insolation through the stomatal function F_1 and the aerodynamic conductance $1/R_a$ that typically follows a similar diurnal profile for its maximum values. Both sites show large ranges of values for the daytime hours because of day-to-day variations in cloud cover (which affects both F_1 and R_a), air temperature (F_4), and wind speed (which also affects R_a). This behavior is different from the ISBA scheme presented by Bouttier et al. (1993a), which varied only by time of day for a particular set of vegetation conditions, with no day-to-day variations. The ISBA scheme was later modified by Giard and Bazile (2000) to include influence of cloud cover, which should result in some degree of day-to-day variations. Note that these modifications result in a hybrid of OI-derived assimilation factors and model-parameter-based factors.

The influence of the quasi-static vegetative parameters, such as LAI, R_{stmin}, and roughness length (implicit through R_a), can be seen in the differences between the grass site and the forest site. In this case, the effects of different LAI and R_{stmin} between the two sites happen to cancel out because at the grass site LAI = 2.5 and $R_{\text{stmin}} = 100$ s m^{-1} while at the forest site LAI = 4.83 and $R_{\text{stmin}} = 200$ s m^{-1}. Thus, the greater maximum values for the forest site were mainly due to greater aerodynamic conductance, resulting from the much greater roughness length ($z_0 = 0.48$ m at the forest site vs $z_0 = 0.07$ m at the grass site).

The relationships between various modeled physical quantities and the deep-soil nudging coefficients for temperature (β_1) are illustrated in Fig. 2. The nudging strength is strongly correlated with parameters that control the coupling between surface conditions and air temperature and humidity. The friction velocity and insolation are strongly correlated with β_1 because they are both directly represented in the β_1 formulation [Eq. (7)]: friction velocity through the aerodynamic resistance term and insolation through the stomatal function F_1. Relationships between β_1 and surface latent heat flux and Bowen ratio are more indirect. Both of these parameters are dependent on the stomatal functions and aerodynamic resistance and are indicators of air–surface coupling. Thus, the correlation with these parameters shows that the β_1 formulation is behaving as intended. Note that the correlation with surface latent heat flux would be stronger if the full formula for bulk stomatal resistance were used in the β_1 definition (including F_2 and F_3, which are functions of deep soil moisture and

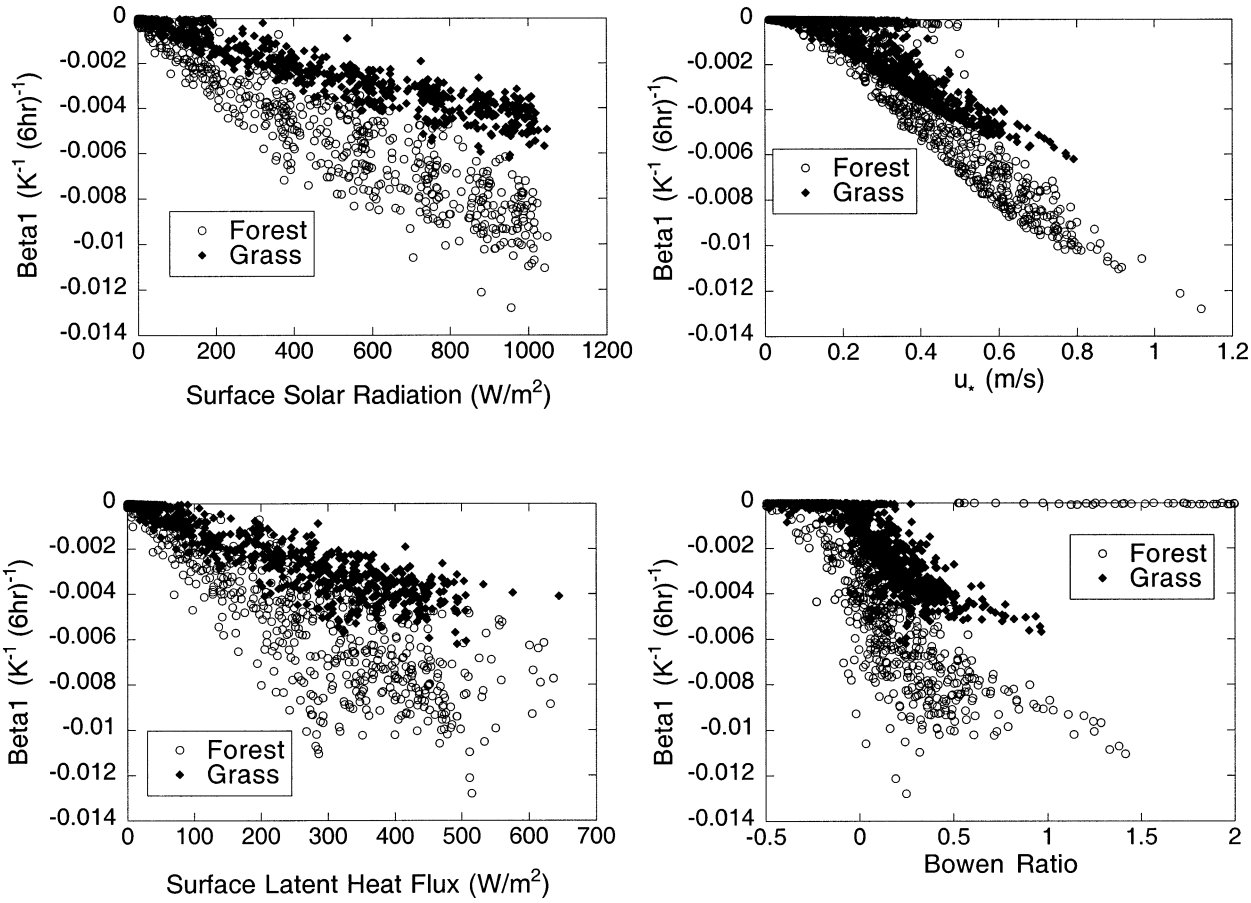

FIG. 2. Deep soil moisture nudging strength for temperature (β_1) related to surface solar radiation, friction velocity, surface latent heat flux, and Bowen ratio.

air humidity). However, that would suppress β_1 at high positive Bowen ratios, which would inhibit nudging effectiveness under dry daytime conditions. This behavior would not be desirable because temperature errors under such conditions could be attributable to erroneous soil moisture values. Also, as discussed above, inhibition of nudging during dry conditions leads to an asymmetrical response that results in exaggerated drying.

Figures 3 and 4 display diurnal temperature biases ($T^a - T^f$) and the corresponding deep-soil-moisture nudging tendencies for the forest and grass sites averaged over the 6-week dataset (note that the scales are different for Figs. 3 and 4). At both sites, the model tends to be consistently too cold when the 2-m model temperature is compared with the observed surface air temperature analyses, particularly in the early evening. Note that some of the nocturnal biases may be attributable to model overprediction of negative (upward) net radiation fluxes. At both sites (Dickson and Franklin, Tennessee), nighttime modeled net radiation was consistently -35 to -40 W m^{-2}, and measurements at these sites were usually -20 to -25 W m^{-2}. As shown in the plots of nudging tendencies, nighttime temperature biases have essentially no effect on the soil moisture nudging, which is fortunate because in this case the radiation errors are probably unrelated to soil moisture. Nighttime temperature biases may be related to soil moisture through its influence on soil heat capacity, but this effect would be confined to a shallow soil layer and, therefore, should not be included in the deep-soil nudging coefficient. We do not attempt to include the heat capacity effect in shallow-layer nudging either because the relationship between air temperature and soil heat capacity is not necessarily a dominant factor. Note that observations of skin temperature, such as from infrared (IR) satellite sensors, may be more amenable to heat capacity assimilation.

At Dickson (Fig. 3), the daytime cool bias averages around 1 K, with the least bias just after noon. Average nudging tendencies differ considerably from the solar diurnal curve, with morning and afternoon peaks but generally stronger nudging in the morning. This pattern reflects the diurnal variation in temperature bias as well as the various parameters that affect the nudging strength. The greater morning nudging tendencies are particularly effective at reducing bias in the peak afternoon temperatures. The negative average nudging tendencies (drying) do not necessarily mean that the

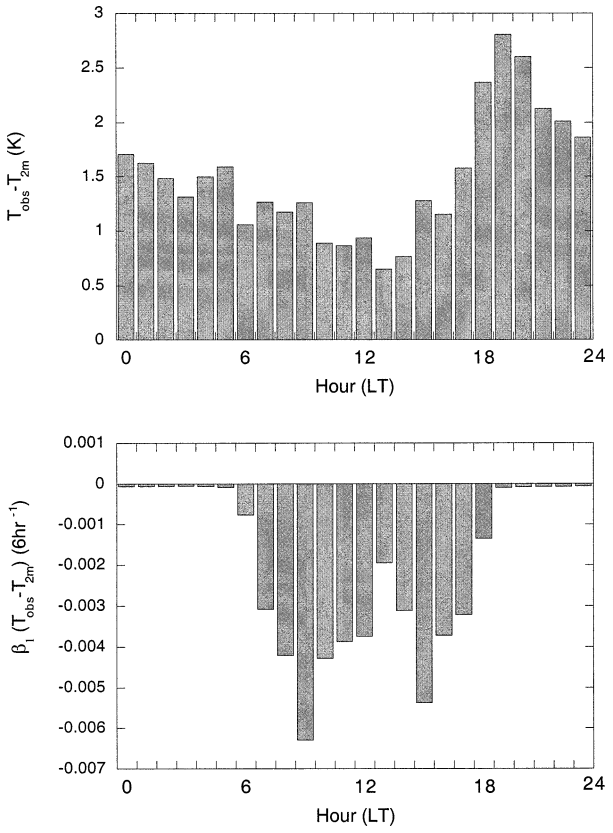

FIG. 3. Diurnal (top) average temperature bias and (bottom) deep soil moisture nudging tendency for a forested site near Dickson, TN.

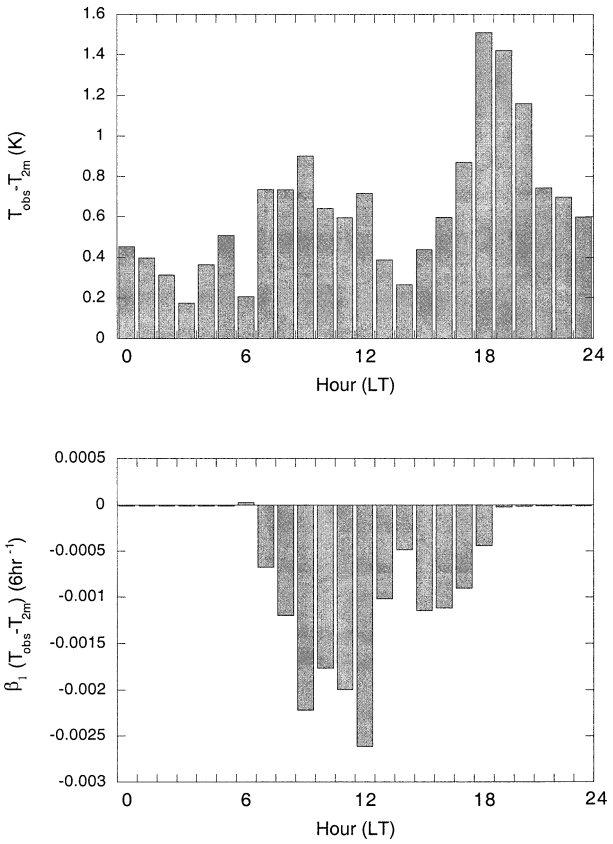

FIG. 4. Diurnal (top) average temperature bias and (bottom) deep soil moisture nudging tendency for a grass site near Franklin, TN.

model would be wetter and cooler if nudging were turned off. The nudging scheme can affect the modeled soil moisture in either direction, thereby working to reduce either warm or cold biases, as will be shown in the next section.

The average temperature bias for the grass site (Fig. 4) is less than 1 K for all but a few early evening hours. Thus, the corresponding nudging tendencies are also very small, with the bulk of it in the morning. The small magnitude of the nudging, however, does not mean that the effect of the nudging scheme is small. On the contrary, the nudging is small because the bias is small as a result of the nudging. An evaluation of the effects of the nudging scheme through comparisons with and without nudging is presented in the next section.

5. Evaluation

The soil moisture nudging scheme is meant to have two primary effects. One is to correct for inadequate initial conditions for soil moisture. The other is to correct continuously for incomplete physics or errors in the LSM or other parts of the model that affect surface fluxes. In this section, each effect is evaluated. The first experiment tests the ability of the model with soil moisture nudging to converge after starting with different initial conditions for soil moisture. The second experiment tests the divergence of model solutions with and without soil moisture nudging starting from the same initial conditions.

We typically use simple initial soil moisture conditions at the start of an extended series of retrospective runs under the assumption that the initial conditions (ICs) will have little impact after a few days of spinup under the influence of soil moisture nudging. To test this assumption, two sets of runs were made, each using simple ICs based on the moisture availability factor M of the dominant land use category in each grid cell and the wilting point w_{wlt}, saturation point w_{sat}, and field capacity w_{fc} appropriate to the soil type in each grid cell. One form gives a relatively wet result:

$$w_2 = M(w_{sat} - w_{wlt}) + w_{wlt}, \quad (8)$$

and the other gives a relatively dry result:

$$w_2 = M(w_{fc} - w_{wlt}) + w_{wlt}. \quad (9)$$

Figure 5 shows the deep soil moisture at several sites in the Nashville, Tennessee, area for both runs. The nudging scheme generally forces convergence in a period of 3–5 days, although, as shown in Fig. 5, the time for convergence can vary considerably from site to site. Convergence can occur in less than 1 day, as for the

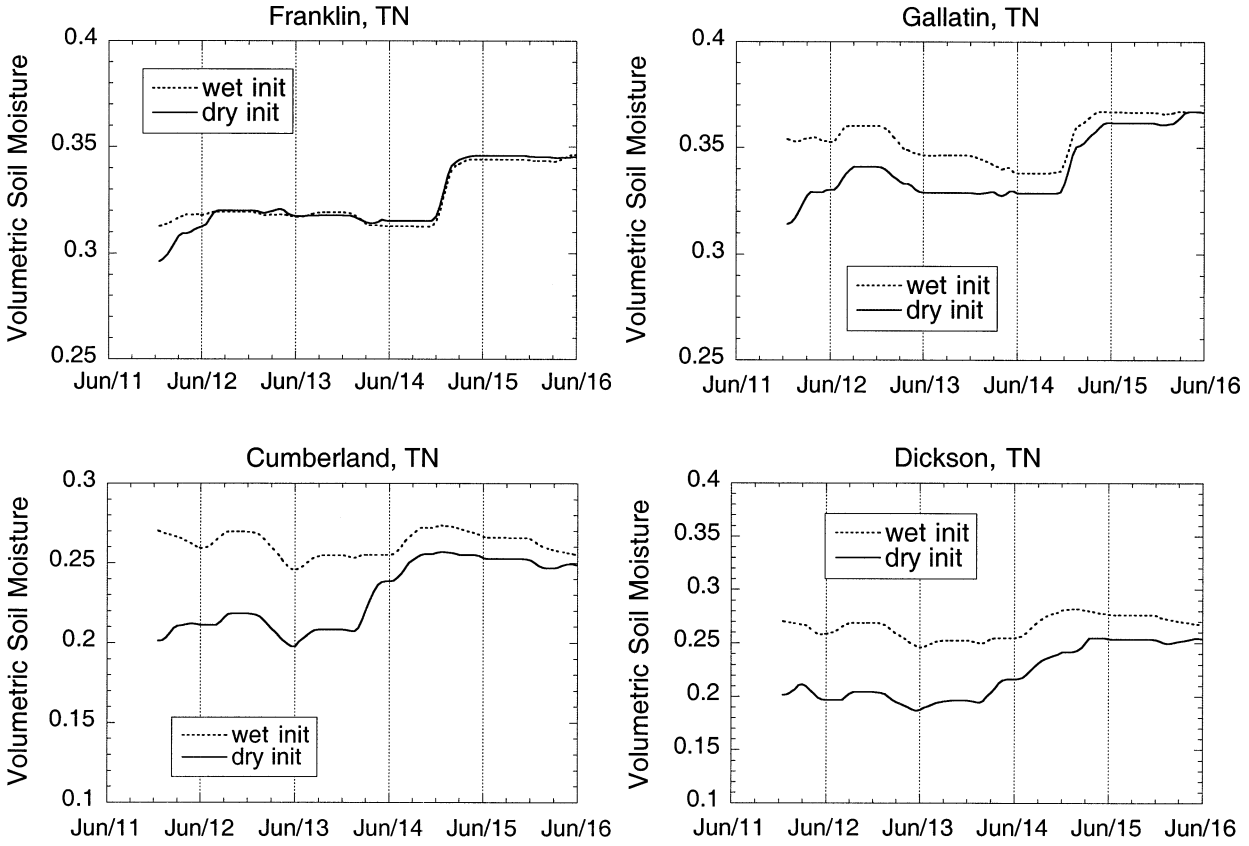

FIG. 5. Deep soil moisture from two sets of initial conditions: wet initialization is according to Eq. (8) and dry initialization is according to Eq. (9).

Franklin site, or take even longer than 5 days, as for the Dickson site.

To test the ability of the nudging scheme to correct for errors caused by the LSM or other parts of MM5 that affect surface air temperature or humidity, we designed an experiment in which the model was run with and without soil moisture nudging and was compared with observations. Both runs started from the same initial conditions for soil moisture and temperature on 13 July after more than 1 month of model simulation with soil moisture nudging. A comparison of modeled and observed 2-m temperature averaged over all surface stations in a 1000 × 1000 km^2 area centered on Nashville is provided in Fig. 6. This area includes 100–130 stations for most hours. After the soil moisture nudging is turned off on 13 July, the nudged and nonnudged simulations produce similar results until they begin to diverge around 21 July. On four of the last five days, the difference in peak temperature is between about 0.5 and 1.0 K, with the nudged simulation closer to the observations (less underprediction).

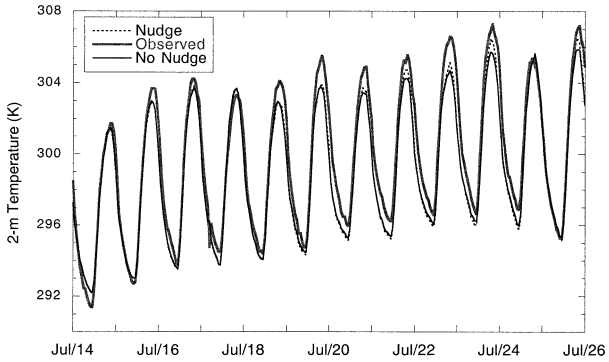

FIG. 6. Modeled and observed 2-m air temperature averaged over all measurement sites within a 1000 km × 1000 km area centered on Nashville, TN.

The differences between the nudged and nonnudged runs are more pronounced when we zoom in on a smaller, more homogeneous region. Figure 7 displays 2-m temperatures averaged over all National Weather Service measurement sites (typically 35–55 stations) within a 680 × 528 km^2 subregion centered on Nashville. This area, extending from northern Mississippi to southern Indiana and most of the east–west extent of Tennessee, was selected to exclude the Mississippi River valley to the west, which has very different soil texture and vegetation, and the corn belt to the north. Figure 7 focuses on the last five days of the simulation, when the model produced considerable precipitation in the analyzed re-

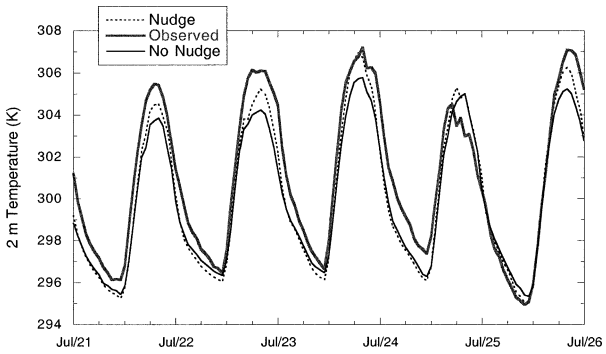

FIG. 7. Same as in Fig. 6 but for a smaller region of 680 km × 528 km centered on Nashville.

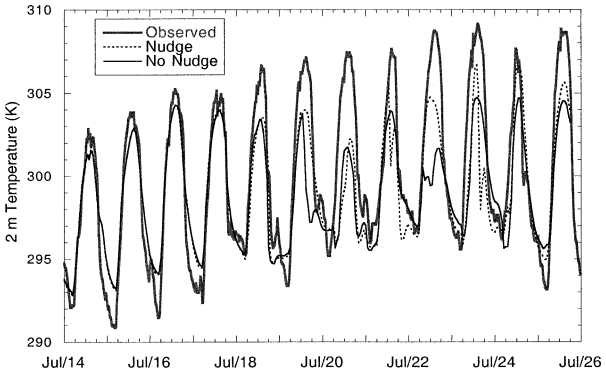

FIG. 9. Modeled and observed 2-m temperature at Keysburg.

gion that was not verified at the observation sites around Nashville. Thus, this is a good example of a situation in which the nudging scheme can produce substantial benefits. On four of the five days, the nudged simulation produced peak averaged temperatures that were about 1 K warmer than the nonnudged run. On all five days, the nudged simulation was within 1 K of the averaged observed values.

To understand further the impact and mechanism of the nudging scheme, hour-by-hour comparisons of soil moisture, 2-m temperature, and surface sensible heat flux are examined at two sites. Figure 8 displays the deep soil moisture (1-m layer) from the two simulations in comparison with observed soil moisture measured at 15-cm depth at a site near Keysburg, Kentucky, (about 60 km northwest of Nashville). This site was agricultural, with both corn and soybeans. Note that because the measurements were uncalibrated, they are plotted against a different scale on the right side of the plot. However, the trends shown by the measurements are realistic. Model predictions and measurements both indicate substantial precipitation early in the period (26 June–3 July) followed by a long drying trend. Right after initiation on 13 July, the nonnudged simulation diverges slightly from the nudged simulation because of a small rain event (not observed) but stays close until 19 July at which time both simulations start to produce substantial amounts of rain (about 10 cm from 19 to 24 July) that were not observed at this site. Without the soil nudging scheme, the rainfall adds to the soil moisture, leading to an increase from 0.26 to 0.34, which is equivalent to about 9 cm of water in this 1-m soil layer. The soil moisture from the simulation with soil moisture nudging continues to decrease through most of this period at an even faster rate during 18–20 July.

The nudging scheme is responding primarily to the underprediction of the 2-m temperature on these days, as illustrated in Fig. 9. Before the rain started, up to 18 July, the model underpredictions are small; therefore, the drying evident in both simulations is due mostly to evapotranspiration, with little effect of the nudging scheme. During most of the rest of the period when the model produces erroneous precipitation, both simulations show substantial underprediction. The nudging scheme responds with strong drying that not only counteracts the moistening effects of the rain but also accelerates the rate of drying. As a result, the simulation with nudging has less underpredition on most of these days. The primary mechanism is that the lower values of root-zone soil moisture restrict the stomatal conduc-

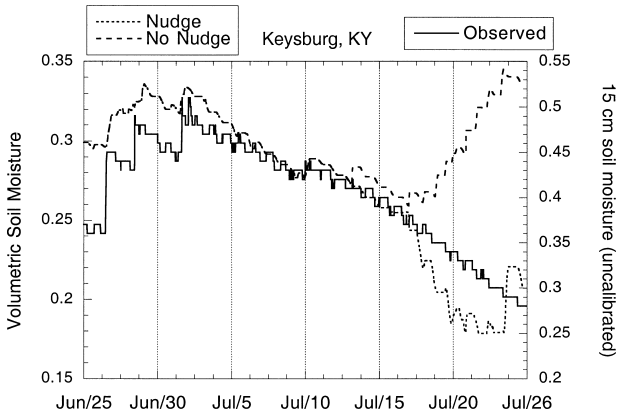

FIG. 8. Modeled deep soil moisture with 15-cm measured soil moisture (uncalibrated) at Keysburg, KY.

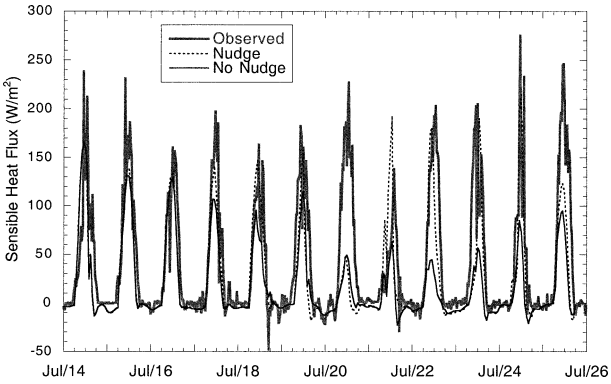

FIG. 10. Modeled and measured surface sensible heat flux at Keysburg.

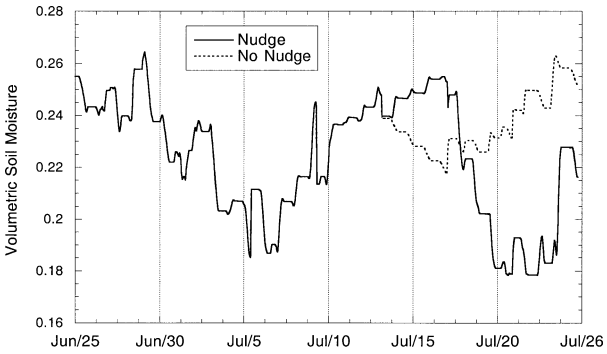

FIG. 11. Modeled deep soil moisture at Dickson.

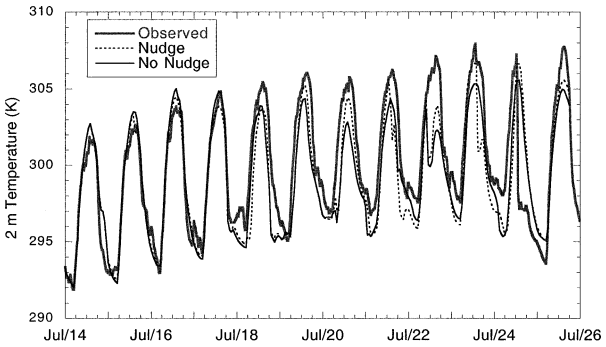

FIG. 12. Modeled and observed 2-m temperature at Dickson.

tance [Eq. (3)] leading to reduced latent heat flux and larger sensible heat fluxes, as depicted in Fig. 10.

Starting on 17 July, the sensible heat flux from the nudged simulation is considerably greater than the nonnudged simulation on all but one day, 20 July, when the model greatly underpredicted net radiation because of excessive cloud cover. Note that on the other days of the modeled rainy period (19–24 July) the modeled net radiation was not underpredicted even though the model had predicted rain when none was observed. This was because all the rain was produced by the subgrid convective parameterization scheme (Kain–Fritsch), which does not directly affect the grid-resolved cloud water (or ice) that is used in the radiation calculation. Another effect of the nudging is a slight reduction of the precipitation from 11 cm for the nonnudged simulation to 9 cm for the nudged run.

This case study shows how the soil moisture nudging scheme can compensate for model errors, such as erroneous precipitation, that are not caused by the LSM. The nudging scheme removed the effects of the fictitious rainfall on the deep soil moisture. Although it also improved the temperature simulation, it could not entirely compensate for the cooling effect of the rain caused by the diversion of surface energy into evaporation from wet canopies and wet ground surface. Even though these immediate improvements were small, the longer-term effect of removing the excessive deep soil moisture is significant.

Figures 11 and 12 display model sensitivity results from another measurement site near Dickson (about 50 km west of Nashville), where forest is the predominant land use. When the nudging was turned off on 13 July, the two simulations diverged immediately. Unlike the Keysburg data, however, the soil moisture increased for the nudged simulation while the nonnudged simulation showed drying for the next four days, typical of clear days with active evapotranspiration in heavily vegetated areas. Beginning on 17 July, the model had predicted rain on most days through 24 July, whereas rain was observed only on 24 July. During the modeled rainy period, the simulation without nudging increased the soil moisture while the nudging produced substantial soil drying for several days. The almost opposite responses of the nudged and nonnudged simulations simply reflect the over- and underpredictions of temperature during the dry and wet periods, as shown in Fig. 12. When the model was not producing precipitation (13–17 July), the nudging increased soil moisture to reduce the model's daytime overprediction of 2-m temperature. During the latter period in which the model produced erroneous rainfall, the nudging dried the soil moisture in response to underprediction of the 2-m temperature caused by evaporation from the rain-wetted canopy and ground. This behavior is similar to the nudging response shown above (Fig. 9) at the Keysburg site during the modeled rainy period. Thus, when the model produces precipitation that is not observed, the nudging tends not only to remove the moistening effect of the rain but also to cause additional drying. Note that on the afternoon of 24 July rain was observed at Dickson with a sharp fall in afternoon temperatures. The model produced rain in the morning but not in the afternoon. The nudging responded by moistening the deep soil during the afternoon when the observed precipitation occurred but not in the morning when the modeled precipitation occurred. Thus, the nudging scheme not only acts to negate the effects of erroneous modeled precipitation but can also fill in for the observed precipitation that the model had missed.

6. Conclusions

Land surface models are becoming increasingly common components of mesoscale meteorological models. Along with the more realistic representation of air–surface interactions come more degrees of freedom for the model. Without a sophisticated method for soil moisture initialization and/or some kind of soil moisture nudging scheme, the addition of an LSM usually degrades the performance of the mesoscale model, particularly the near-surface air temperature. The two most common approaches to this problem are use of an ''offline'' model, usually known as a land data assimilation system (LDAS), or an ''online'' system such as the indirect nudging scheme described here. The LDAS approach

is essentially continuous running of an LSM outside of the mesoscale model, driven by observed meteorological fields, that then provides soil moisture fields for initialization of the LSM within the mesoscale model. The main advantage of this approach is that the observed fields of precipitation and solar radiation are directly assimilated into the LDAS, eliminating soil moisture errors caused by errors in these modeled fields. The obvious disadvantage is that the LDAS is an additional major model and data assimilation system. The online approach is much simpler and less resource-intensive. As shown in section 5, the nudging scheme can very effectively and quickly spin up appropriate initial soil moisture fields. Nudging can also effectively counteract erroneous model precipitation, as demonstrated in section 5. This ability to correct for the effects of model errors during simulation is a clear advantage over the LDAS approach that is particularly valuable for extended retrospective modeling for air-quality simulations.

A third approach is variational assimilation of 2-m observations to produce soil moisture analyses, as described by Mahfouf (1991) and Hess (2001). The technique for assimilation of 2-m temperature described by Hess (2001) has recently become operational in a German NWP model. These techniques are similar to the nudging scheme presented here, as well as the OI schemes, in that they use model errors in comparison with 2-m observations to modify soil moisture. Variational schemes have been shown to produce very good results, but they involve considerably more computational expense than nudging schemes do. These schemes may be particularly attractive in model systems that use 4D variational techniques operationally, because, they involve integration in time.

Model errors in surface radiation can cause particular difficulties for the nudging scheme, because radiation errors can cause significant temperature errors that are unrelated to soil moisture. Thus, the nudging scheme will change the soil moisture in these situations, which may add errors during subsequent simulation hours. The situation in which the model overpredicts cloud cover and, therefore, underpredicts surface solar radiation is amedliorated by the formulation of the nudging coefficient that includes a functional dependence on solar radiation. When the modeled solar radiation is low, the nudging strength in low. However, the converse situation, in which the model underpredicts the cloud cover, is more problematic because the nudging strength will be high when the modeled solar radiation is high. We have often seen periods of temperature underprediction following periods of underpredicted cloud cover when nudging increased soil moisture. Although the model usually recovers quickly, such cloud-cover errors can cause the nudging scheme to add a cold bias for about two days. Douville et al. (2000) noted similar asymmetric response to model errors in cloud cover in the OI scheme modified by Giard and Bazile (2000) to include an empirical function of cloud cover. Techniques for direct assimilation of surface solar radiation estimates such as are derived from Geostationary Operational Environmental Satellite imagery promise to improve this problem greatly (McNider et al. 1998). Thus, assimilation of observed radiation and possibly precipitation fields directly into mesoscale models along with online nudging could add the advantages of the LDAS approaches to the simplicity and efficiency of online systems.

Acknowledgments. We thank Dr. Tilden Meyers of NOAA/ATDD in Oak Ridge, Tennessee, for providing surface flux measurements at Keysburg and Franklin.

REFERENCES

Benjamin, S. G., and N. L. Seaman, 1985: A simple scheme for objective analysis in curved flow. *Mon. Wea. Rev.,* **113,** 1184–1198.

Blackadar, A. K., 1978: Modeling pollutant transfer during daytime convection. Preprints, *Fourth Symp. on Atmospheric Turbulence, Diffusion, and Air Quality,* Reno, NV, Amer. Meteor. Soc., 443–447.

Bouttier, F., J. F. Mahfouf, and J. Noilhan, 1993a: Sequential assimilation of soil moisture from atmospheric low-level parameters. Part I: Sensitivity and calibration studies. *J. Appl. Meteor.,* **32,** 1335–1351.

——, ——, and ——, 1993b: Sequential assimilation of soil moisture from atmospheric low-level parameters. Part II: Implementation in a mesoscale model. *J. Appl. Meteor.,* **32,** 1352–1364.

Chen, F., and J. Dudhia, 2001: Coupling an advanced land surface–hydrology model with the Penn State–NCAR MM5 modeling system. Part I: Model implementation and sensitivity. *Mon. Wea. Rev.,* **129,** 569–604.

Douville, H., P. Viterbo, J. F. Mahfouf, and A. C. M. Beljaars, 2000: Evaluation of the optimum interpolation and nudging techniques for soil moisture analysis using FIFE data. *Mon. Wea. Rev.,* **128,** 1733–1756.

Giard, D., and E. Bazile, 2000: Implementation of a new assimilation scheme for soil and surface variables in a global NWP model. *Mon. Wea. Rev.,* **128,** 997–1015.

Grell, G. A., J. Dudhia, and D. R. Stauffer, 1994: A description of the fifth-generation Penn State/NCAR Mesoscale Model (MM5). NCAR Tech. Note NCAR/TN-398+STR, 122 pp.

Hess, R., 2001: Assimilation of screen-level observations by variational soil moisture analysis. *Meteor. Atmos. Phys.,* **77,** 145–154.

Holtslag, A. A. M., E. V. Meijgaard, and W. C. DeRooy, 1995: A comparison of boundary layer diffusion schemes in unstable conditions over land. *Bound.-Layer Meteor.,* **76,** 69–95.

Jacquemin, B., and J. Noilhan, 1990: Sensitivity study and validation of a land surface parameterization using the HAPEX–MOBILHY data set. *Bound.-Layer Meteor.,* **52,** 93–134.

Kain, J. S., and J. M. Fritsch, 1990: A one-dimensional entraining/detraining plume model and its application in convective parameterization. *J. Atmos. Sci.,* **47,** 2784–2802.

——, and ——, 1993: Convective parameterization for mesoscale models: The Kain–Fritsch scheme. *The Representation of Cumulus Convection in Numerical Models, Meteor. Monogr.,* No. 46, Amer. Meteor. Soc., 165–170.

Mahfouf, J.-F., 1991: Analysis of soil moisture from near-surface parameters: A feasibility study. *J. Appl. Meteor.,* **30,** 1534–1547.

McNider, R. T., W. B. Norris, D. Casey, J. E. Pleim, S. J. Roselle, and W. M. Lapenta, 1998: Assimilation of satellite data in regional air quality models. *Air Pollution Modeling and Its Ap-*

plication XII, S.-E. Gryning and N. Chaumerliac, Eds., Plenum Press, 25–35.

Mlawer, E. J., S. J. Taubman, P. D. Brown, M. J. Iacono, and S. A. Clough, 1997: Radiative transfer for inhomogeneous atmospheres: RRTM, a validated correlated-*k* model for longwave. *J. Geophys. Res.,* **102,** 16 663–16 682.

Noilhan, J., and S. Planton, 1989: A simple parameterization of land surface processes for meteorological models. *Mon. Wea. Rev.*, **117,** 536–549.

Pleim, J. E., 1999: Modeling stomatal response to atmospheric humidity. Preprints, *13th Symp. on Boundary Layers and Turbulence*, Dallas, TX, Amer. Meteor. Soc., 291–294.

——, and J. S. Chang, 1992: A non-local closure model for vertical mixing in the convective boundary layer. *Atmos. Environ.,* **26A,** 965–981.

——, and A. Xiu, 1995: Development and testing of a surface flux and planetary boundary layer model for application in mesoscale models. *J. Appl. Meteor.,* **34,** 16–32.

——, and ——, 2001: Updates and evaluation of the PX-LSM in MM5. Preprints, *11th PSU/NCAR Mesoscale Model User's Workshop*, Boulder, CO, National Center for Atmospheric Research, 98–101.

——, ——, P. L. Finkelstein, and T. L. Otte, 2001: A coupled land-surface and dry deposition model and comparison to field measurements of surface heat, moisture, and ozone fluxes. *Water Air Soil Pollut. Focus,* **1,** 243–252.

Reisner, J., R. M. Rasmussen, and R. T. Bruintjes, 1998: Explicit forecasting of supercooled liquid water in winter storms using the MM5 mesoscale model. *Quart. J. Roy. Meteor. Soc.,* **124B,** 1071–1107.

Stauffer, D. R., and N. L. Seaman, 1990: Use of four-dimensional data assimilation in a limited-area mesoscale model. Part I: Experiments with synoptic-scale data. *Mon. Wea. Rev.,* **118,** 1250–1277.

——, ——, and F. S. Binkowski, 1991: Use of four-dimensional data assimilation in a limited-area mesoscale model. Part II: Effects of data assimilation within the planetary boundary layer. *Mon. Wea. Rev.,* **119,** 734–754.

Xiu, A., and J. E. Pleim, 2001: Development of a land surface model. Part I: Application in a mesoscale meteorological model. *J. Appl. Meteor.,* **40,** 192–209.